Cell Reports, Volume *37*

Supplemental information

Interplay between protein acetylation and ubiquitination controls MCL1 protein stability

Kouhei Shimizu, Min Gi, Shugo Suzuki, Brian J. North, Asami Watahiki, Satoshi Fukumoto, John M. Asara, Fuminori Tokunaga, Wenyi Wei, and Hiroyuki Inuzuka

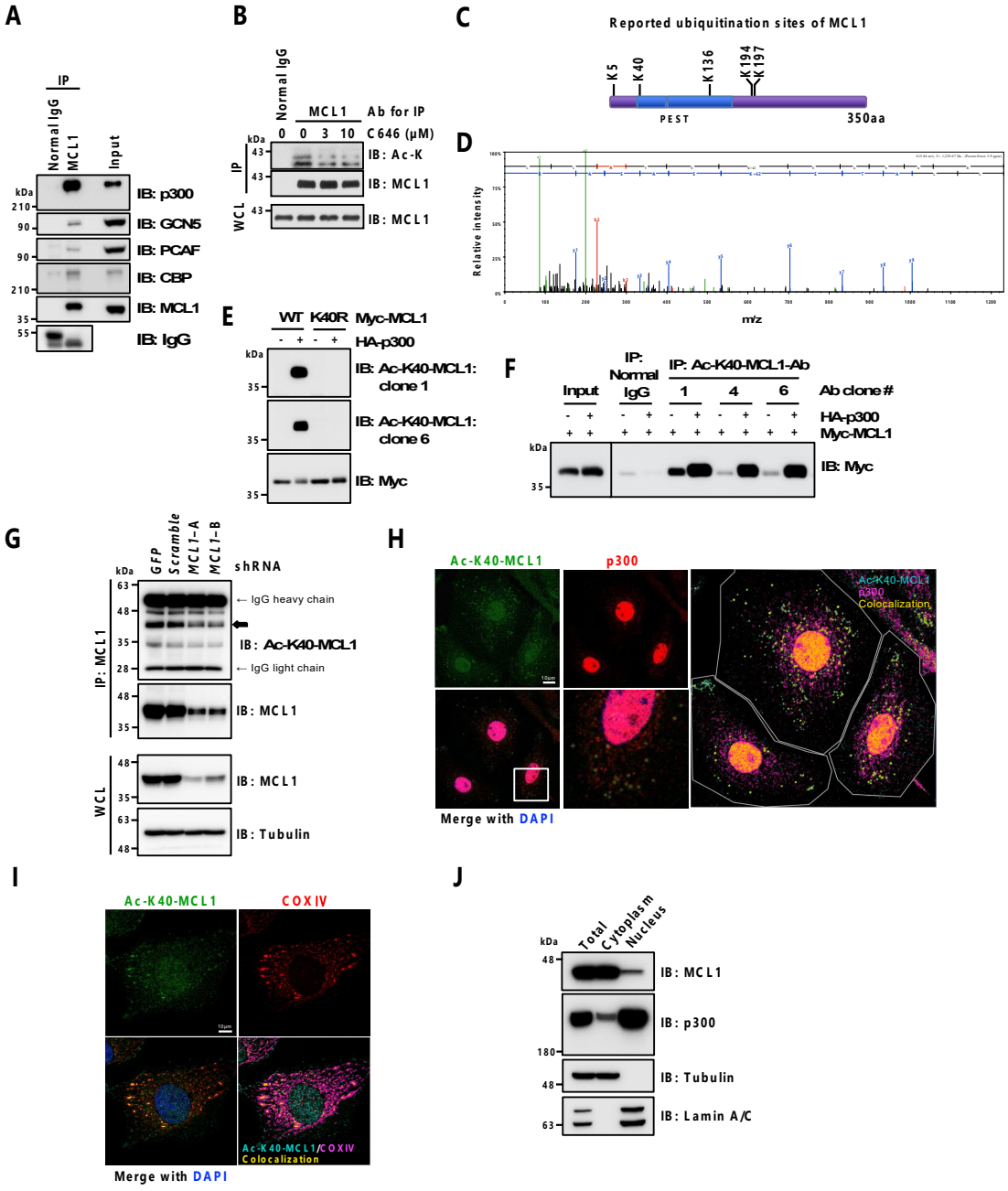

Figure S1. p300 binds and acetylates MCL1 at the lysine 40 (K40) residue, related to Figure 1.

A, Evaluation of endogenous interaction between MCL1 and the indicated lysine acetyltransferases. Immunoblot (IB) analysis of whole-cell lysates (WCL) (input: 60 μg of cell lysates) and anti-MCL1 immunoprecipitates (IP) derived from HeLa cells.

B, Treatment with the p300/CBP inhibitor C646 reduces the MCL1 acetylation. IB analysis of WCL and anti-MCL1 IP derived from HeLa cells. The cells were treated overnight with C646 at the indicated concentration before harvesting.

C, A schematic diagram of reported ubiquitination sites in MCL1.

D, The LC-MS/MS spectrum for peptide LLATEkEASAR shows the location of acetylation at Lys40 in the human MCL1 protein via the +42 Da shift from the y5 to y6 fragment ions.

E, IB analysis of WCL derived from 293T cells transfected with the Myc-MCL1 constructs together with HA-p300 as indicated. Cells were harvested at 48 h after transfection.

F, IB analysis of anti-acetylated (Ac)-K40-MCL1-IP derived from 293T cells transfected with Myc-MCL1 and HA-p300 constructs as indicated. Cells were harvested at 48 h after transfection for IP.

G, IB analysis of WCL and anti-MCL1-IP derived from SKBR3 cells stably expressing the lentiviral shRNA specific for *GFP, Scramble,* or *MCL1*(using two independent shRNAs).

H, Endogenous acetylated-K40 (Ac-K40) MCL1 colocalizes with the p300 acetyltransferase in the nucleus and cytoplasm of BT-20 breast cancer cells. Immunofluorescence (IF) images of Ac-K40-MCL1 (green) and p300 (red) with DAPI staining (blue) in BT-20 cells. Scale bar, 10 μm.

I, Endogenous Ac-K40-MCL1 is present in mitochondria of BT-20 breast cancer cells. Immunofluorescence (IF) images of Ac-K40-MCL1 (green) and COX IV (red), a mitochondrial marker protein, with DAPI staining (blue) in BT-20 cells. Scale bar, 10 μm.

J, IB analysis of WCL, cytoplasmic and nuclear extracts derived from HeLa cells.

Data (A), (B), (E)-(G), and (J) are representative of at least two independent experiments.

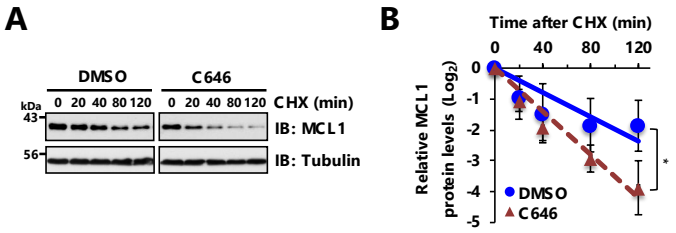

Figure S2. p300-mediated MCL1 acetylation leads to MCL1 stabilization in part through decreasing MCL1 ubiquitination, related to Figure 2.

A, Treatment with the p300/CBP inhibitor C646 shortens MCL1 protein half-life. IB analysis of WCL derived from PF382 cells. Cells were pretreated with C646 (10 μM) overnight and then treated with 100 μg/mL cycloheximide (CHX) for the periods indicated before harvesting.

B, Quantification of the MCL1 band intensities of IB replicates of (**A**). Data are presented as the mean ± SD; n = 3 independent experiments, * $p < 0.05$.

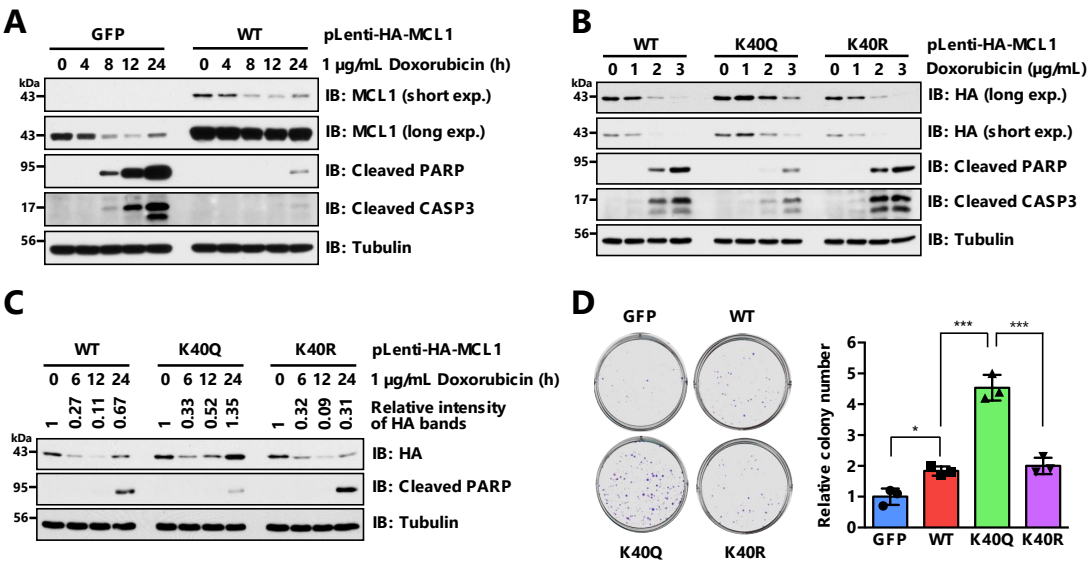

Figure S3. Acetylation-mimetic MCL1 K40Q displays enhanced anti-apoptotic function and oncogenicity, related to Figure 3.

A-C, Acetylation-mimetic MCL1 K40Q exerts enhanced anti-apoptotic function. IB analysis of WCL derived from HeLa cells stably expressing GFP (as a control) or HA-MCL1 (WT, K40Q, or K40R). Cells were treated with doxorubicin for the time period indicated at 1 μg/mL (**A** and **C**) or at the indicated concentration for 24 h (**B**).

D, Acetylation-mimetic MCL1 K40Q enhances colony formation potential of HeLa cells. Colony-formation assay was conducted using HeLa cells presented in (**A-C**). These cells were pretreated overnight with doxorubicin (0.02 μg/mL) before plating for the assays. Data are presented as the mean ± SD; n = 3 biological replicates, * $p < 0.05$, *** $p < 0.001$.

Data (A)-(C) are representative of at least two independent experiments.

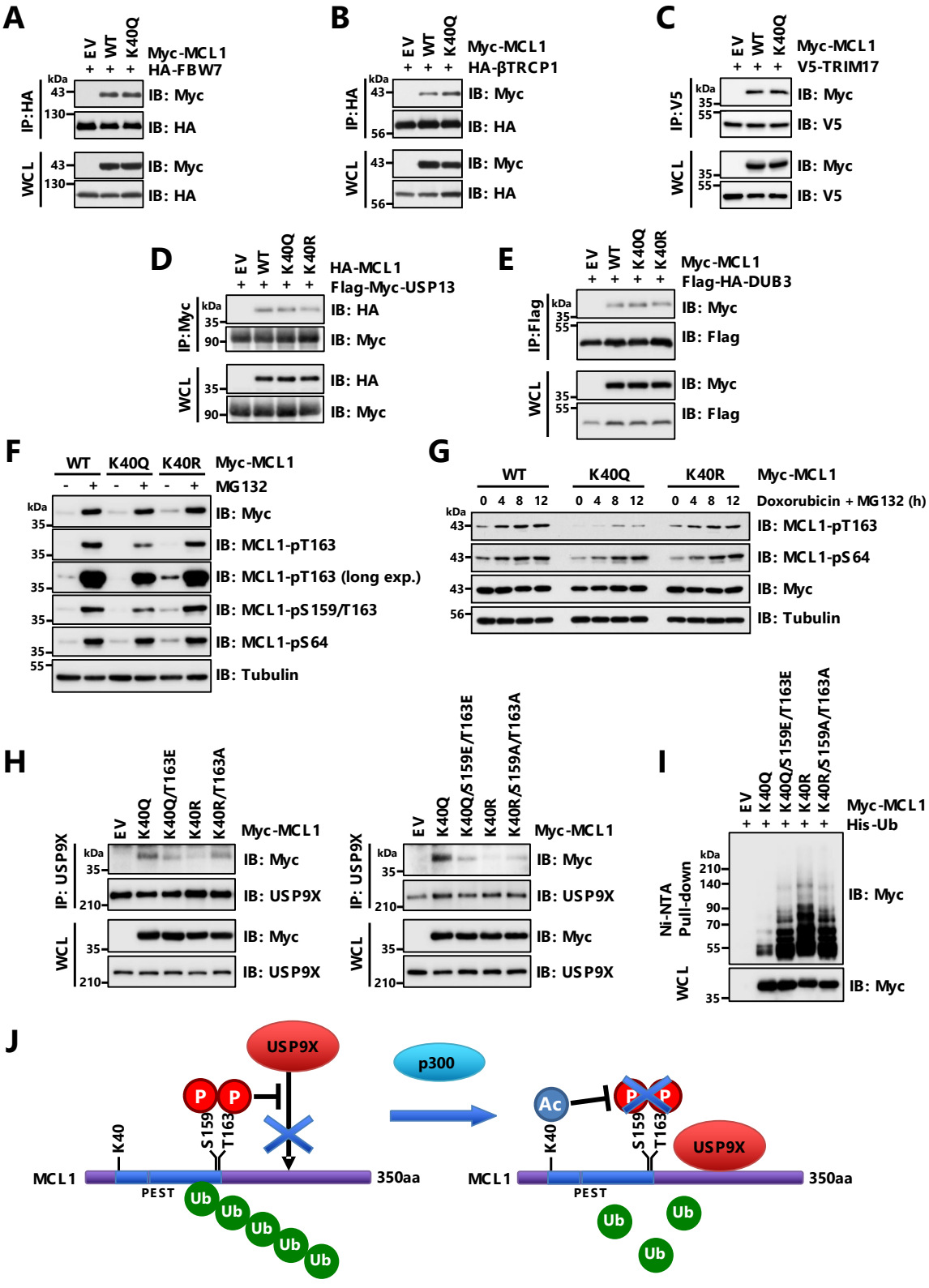
A
EV
WT
K40Q
Myc-MCL1
HA-FBW7
IP:HA
WCL
IB: Myc
IB: HA
B
Myc-MCL1
HA-βTRCP1
C
Myc-MCL1
V5-TRIM17
IP:V5
IB: V5
D
K40R
HA-MCL1
Flag-Myc-USP13
IP:Myc
E
Myc-MCL1
Flag-HA-DUB3
IP:Flag
IB: Flag
F
MG132
IB: MCL1-pT163
IB: MCL1-pT163 (long exp.)
IB: MCL1-pS159/T163
IB: MCL1-pS64
IB: Tubulin
G
Doxorubicin + MG132 (h)
IB: MCL1-pT163
IB: MCL1-pS64
H
K40Q/T163E
K40R/T163A
K40Q/S159E/T163E
K40R/S159A/T163A
IP: USP9X
IB: USP9X
I
His-Ub
Ni-NTA Pull-down
J
USP9X
p300
MCL1
350aa
PEST
K40
S159
T163
Ub
Ac
P

Figure S4. MCL1 acetylation promotes its interaction with USP9X, resulting in MCL1 deubiquitination and stabilization, related to Figure 4.

A-E, IB analysis of WCL and anti-HA, anti-V5, anti-Myc, or anti-Flag IP derived from 293T cells transfected with the indicted constructs. At 36 h after transfection, cells were treated overnight with MG132 (10 μM) before harvesting for IP.

F, The acetylation-mimetic K40Q mutation impairs MCL1 phosphorylation at S159/T163. IB analysis of WCL derived from CRISPR/Cas9-mediated *MCL1*-knockout HeLa cells transfected with the indicated Myc-MCL1 constructs. At 36 h after transfection, cells were treated with MG132 (10 μM) for 12 h before harvesting.

G, IB analysis of WCL derived from HeLa cells transfected with the indicated Myc-MCL1 constructs. At 36 h after transfection, cells were co-treated with doxorubicin (1 μg/mL) and MG132 (15 μM) for the periods indicated before harvesting.

H, Phosphorylation-mimetic S159E/T163E mutations impair the interaction of MCL1 with USP9X regardless of the acetylation-mimetic K40Q mutation. IB analysis of WCL and anti-USP9X IP derived from CRICPR/Cas9-mediated *MCL1*-knockout HCT116 cells transfected with the indicated Myc-MCL1 constructs. At 36 h after transfection, cells were treated overnight with MG132 (10 μM) before harvesting for IP.

I, Additive phosphorylation-mimetic S159E/T163E mutations restore the ubiquitination of acetylation-mimetic MCL1 K40Q. 293T cells were transfected with the indicated Myc-MCL1 and His-ubiquitin (His-Ub) constructs. At 36 h after transfection, cells were treated overnight with MG132 (10 μM) before harvesting. His-Ub-conjugated proteins were captured with Ni-NTA agarose beads and subjected to IB analysis.

J, A schematic diagram of the crosstalk between phosphorylation at S159/T163 and acetylation at K40 of the MCL1 protein in regulating MCL1 interaction with USP9X.

Data (A)-(I) are representative of at least two independent experiments.

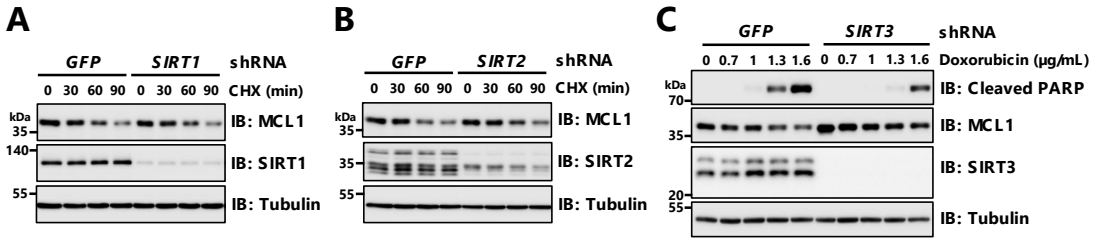

Figure S5. SIRT3 negatively regulates MCL1 protein stability through deacetylation of MCL1, related to Figure 5.

A and B, *SIRT1* or *SIRT2* depletion shows minimal effects on MCL1 protein half-life. IB analysis of WCL derived from HeLa cells stably expressing the lentiviral shRNA specific for *GFP*, *SIRT1*, or *SIRT2*. Cells were treated with 100 μg/mL CHX for the period indicated before harvesting.

C, *SIRT3* depletion desensitizes cells to doxorubicin through MCL1 stabilization. IB analysis of WCL derived from HeLa cells stably expressing the lentiviral shRNA specific for *GFP* or *SIRT3*. Cells were treated with the indicated concentrations of doxorubicin for 24 h before harvesting.

Data (A)-(C) are representative of at least two independent experiments.

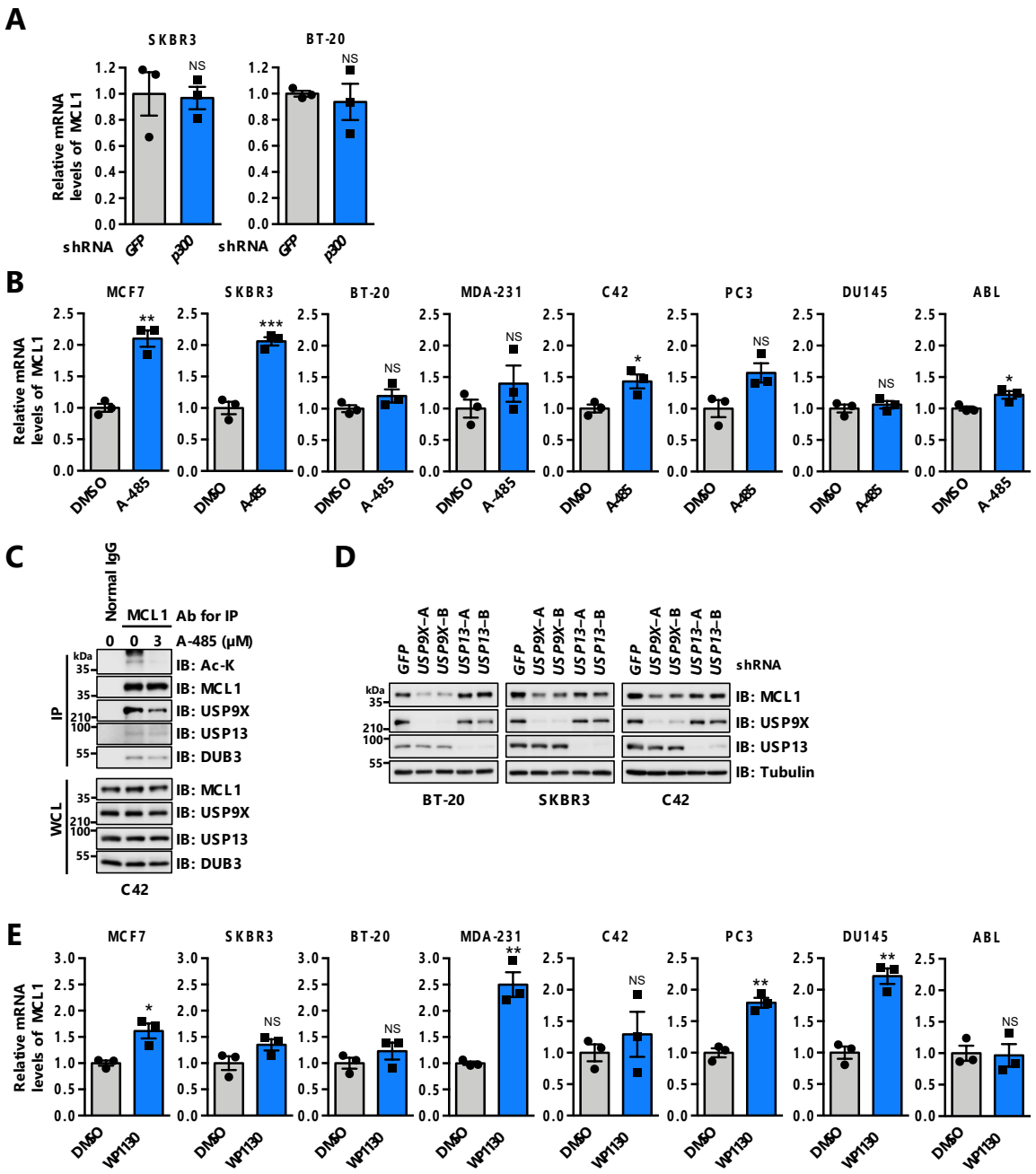

Figure S6. MCL1 acetylation promotes cancer cell survival in a p300 and USP9X dependent manner, related to Figure 6.

A, Real-time RT-PCR analysis to determine the relative mRNA expression levels of MCL1 in SKBR3 and BT-20 cells presented in Figure 6B. *GAPDH* was utilized for normalization. Data are presented as the mean ± SEM, n = 3 biological replicates, NS: not significant.

B, Real-time RT-PCR analysis to determine the relative mRNA expression levels of MCL1 in breast and prostate cancer cells presented in Figure 6C. These cells were treated with A-485 (3 μM) for 48 h before harvesting. *GAPDH* was utilized for normalization. Data are presented as the mean ± SEM, n = 3 biological replicates, * $p < 0.05$, ** $p < 0.01$, *** $p < 0.001$, NS: not significant.

C, Treatment with the p300/CBP inhibitor A-485 reduces MCL1 acetylation and promotes dissociation of USP9X from MCL1. IB analysis of WCL and anti-MCL1 IP derived from C42 cells treated overnight with A-485 at the indicated concentration before harvesting.

D, *USP9X* depletion reduces MCL1 protein levels in the indicated breast and prostate cancer cells. IB analysis of WCL derived from BT-20, SKBR3, and C42 cells stably expressing the lentiviral shRNA specific for *GFP*, *USP9X*, or *USP13*.

E, Real-time RT-PCR analysis to determine the relative mRNA expression levels of *MCL1* in breast and prostate cancer cells presented in Figure 6G-H. These cells were treated with WP1130 (3 μM) for 8 h (breast cancer cells) or 12 h (prostate cancer cells) before harvesting. *GAPDH* was utilized for normalization. Data are presented as the mean ± SEM, n = 3 biological replicates, * $p < 0.05$, ** $p < 0.01$, NS: not significant.

Data (C) and (D) are representative of at least two independent experiments.